JBAT 13(2) (2024) 117 – 129

Jurnal Bahan Alam Terbarukan

Accredited SINTA 2 by Ministry of Research and Technology/National Research and Innovation Agency
SK No. 200/M/KPT/2020
http://journal.unnes.ac.id/nju/index.php/jbat

p-ISSN 2303 0623
e-ISSN 2407 2370

Effect of Heating Time Variation on The Activation of Modified Palm Oil Fly Ash as β-Carotene Adsorbent on Crude Palm Oil

Simparmin Br. Ginting[1], Sona Erlangga[1,✉], Heri Rustamaji[1], Darmansyah[1],Muhammad Niki Wijaya[1], Herry Wardono[2]

DOI: https://doi.org/10.15294/jbat.v13i2.9742

[1] Chemical Engineering Department, Faculty of Engineering, University of Lampung, Bandar Lampung, 35141, Indonesia
[2] Mechanical Engineering Department, Faculty of Engineering, University of Lampung, Bandar Lampung, 35141, Indonesia

Article Info

Article history:
Received
16 July 2024
Revised
9 November 2024
Accepted
4 December 2024
Published
December 2024

Keywords:
Activation;
Adsorption;
β-carotene;
CPO ;
Impregnation;
POFA

Abstract

Crude Palm Oil (CPO) contains β-carotene as source of pro-vitamin A. Alternative adsorbent that can be used to adsorb β-carotene is Palm Oil Fly Ash (POFA). This study aims to determine the ability of POFA activated with H_3PO_4 and Cu/Zn impregnation to adsorb β-carotene from CPO to obtain characteristics data of modified POFA and its ability to adsorb β-carotene. The main materials used were CPO and POFA. The parameters observed were the characterization and performance test of 9% H_3PO_4-activated POFA produced at various heating times for 90, 150, and 210 minutes with Cu/Zn impregnation. BET analysis showed the POFA with heating time of 90 minutes had the largest surface area of 19.4785 m^2/g, XRD showed the presence of CuO, ZnO, quartz, and SiO2 diffraction patterns, FTIR showed that the POFA contained O-H groups, O-H, Si-H, Al-O, asymmetric Si-O, and Si-O-Si bending vibrations, and SEM-EDX results showed that POFA has hollow pores and a rough spherical surface. Based on the results of UV-Vis Spectrophotometry analysis, the most optimal result was obtained in the β-carotene adsorption process with POFA-modified 2 variations of activation heating time for 150 minutes, which succeeded in adsorbing 86% of β-carotene.

INTRODUCTION

Crude Palm Oil (CPO), which naturally contains retinol, is a rich source of carotenoids (pro-vitamin A). Carotenoids, which give palm oil its characteristic red color, are present in CPO at levels of 500-700 ppm. β-carotene (60-65%) in the carotenoid relative is the main cause of the red color (Okogeri & Okoro, 2014).

Extraction, saponification, transesterification and adsorption are some of the previously documented techniques to remove carotenoids from palm oil (Choo, 2000). Saponification uses a strong acid base that reacts with triglycerides that hydrolyze to form soap and is able to separate bioactive compounds (unsaponifiable fraction). One example of bioactive compounds is carotenoids. Methyl esters containing carotenoids that are formed from triglycerides in the transesterification process will form in the upper layer, and in the lower layer will form glycerol due to differences in density. Saponification and transesterification methods only separate carotenoids from several other fractions but the results do not only contain carotenoids, so an extraction method is needed. Because carotenoids are non-polar, the extraction method used for carotenoid retrieval uses non-polar solvents so that

✉ Corresponding author:
E-mail: sonaerlangga03@gmail.com

a bond between carotenoids and the solvent or carotenoid substances can dissolve. The adsorption method of carotenoids from CPO will use adsorbents that have bonds with carotenoids or have a large surface area. One of the adsorbents that can be used to extract β-carotene from CPO is industrial waste such as palm kernel shell waste which is one of the alternative adsorbents that has a lot of potential. For boiler engines, this waste is often used as fuel (Rasmawan, 2009).

The boiler combustion process will produce ash from palm kernel shells that has a melting point higher than the combustion temperature. Fly ash has a much finer in texture, lighter in hue, and darker in color than bottom ash, this material is called Palm Oil Fly Ash (POFA). Due to its high SiO_2 content (up to 55.1%), POFA performs well as an adsorbent making it capable of reducing the amount of β-carotene in CPO (Yahya et al., 2013). POFA pollutants are removed through chemical activation using Phosphoric Acid (H_3PO_4). This is because the more H^+ ions that enter the POFA structure, the more impurities are collected so that active Bronsted acid groups are formed which easily release protons in the POFA (Irawan, 2013).

The surface area of activated carbon produced is affected by the activation temperature used. The surface area also depends on how long the activation process takes. This shows that the surface area of activated carbon can vary depending on the influence of the technique, duration and temperature of the activation process used (Shofa, 2012). Activated carbon is made from palm shell waste which has been activated with H_3PO_4 in various concentrations of 1, 3, 5, 7 and 9% at temperature of 110°C. Carbonization takes place for ½ hours at 400°C to produced palm shell activated carbon. The activated carbon is really good and shiny black in color. Soaking in H_3PO_4 9% for 22 hours is the ideal activation environment (Elly, 2008).

Rice husk biosilica extraction waste can be used as an adsorbent. The method for activating the dregs left over from biosilica extraction uses $ZnCl_2$, H_3PO_4, and KOH. The results of this research show that the synthesis of adsorbents through the impregnation process produces the highest surface area and iodine absorption capacity, namely 24.32 mg/g and 1281.65 m^2/g using the activating agent H_3PO_4. The characteristics of the adsorbent meet the SNI requirements (Rahayu et al., 2021).

The production and characterization of silica-alumina (SA) which functions as a Cu/Zn metal oxide catalyst substrate. The Cu/Zn/SA mixed metal oxide catalyst was prepared using an impregnation technique. Functional group analysis (FTIR) revealed that SiOH, Al-OH, and OH were the dominant species in SA. CuO and ZnO metal oxides produced in SA were found in significant quantities (Hosseini et al., 2015).

According to some previous studies, adsorption results with POFA have been favorable for adsorbing β-carotene content from CPO. The active side on the adsorbent surface can also be enhanced by impregnation of $Cu(NO_3)_2.3H_2O$ metal with $ZnSO_4.7H_2O$ promoter. Cu^{2+} can bind to β-carotene (Gao & Kispert, 2014). Therefore, to adsorb β-carotene from CPO, POFA adsorbent from palm kernel shell combustion activated with H_3PO_4 and impregnated with metal $Cu(NO_3)_2.3H_2O$ with $ZnSO_4.7H_2O$ promoter was used in this study. The activation process requires different heating durations as an important comparative factor in determining the adsorption ability due to the diverse material quality (Shofa, 2012).

This study aims to determine the characteristics of POFA activated with H_3PO_4 9% concentration at various of heating time for 90, 150 and 210 minutes, then impregnated with Cu/Zn which is analyzed using BET, SEM-EDX, FTIR and XRD analysis. Apart from that, it is also to determine the effect of heating activation time on ability of modified POFA in adsorbing β-carotene.

METHODS

The method in this research referred to the method previously carried out by (Elly, 2008; Harahap et al., 2020; Ho et al., 2012; Hosseini et al., 2015; Rangkuti et al., 2021; Wardhani & Aini, 2016). The stages in producing modified POFA were conducted using the activation method, with heating times varied at 90, 150, and 210 minutes. Following this step, the sample was converted to activated POFA, which was then impregnated. After this process, modified POFA was obtained and subsequently used to adsorb β-carotene in batches using the immersion method.

Palm Oil Fly Ash (POFA) Sample Preparation

POFA is dried in the sun for one day. Then it was crushed using a mortar and filtered using a

200 mesh sieve and then the sample weighed 12 g using an analytical balance.

POFA Activation Uses H_3PO_4 9%

12 g of refined POFA was soaked in 30 mL of H_3PO_4 9% solution in a closed beaker glass covered with aluminum foil for 24 hours. After the soaking process is complete, the sample is filtered with filter paper and neutralized to a neutral pH (pH = 6/7) using distilled water. The samples were then dried using an oven at 110°C with various heating time of 90, 150, and 210 minutes. The purpose of selecting the heating time ratio is to determine its effect on the characteristics of activated POFA. After the activation process, three samples were obtained, namely POFA-activated 1, POFA-activated 2, and POFA-activated 3, then continued with the adsorbent impregnation stage.

Preparation of Impregnant Solution

The impregnant solution was prepared by mixing $Cu(NO_3)_2.3H_2O$ (99.5%, Friendemann-Schmidt) and $ZnSO_4.7H_2O$ (> 99%, Sigma–Aldrich). The solution was prepared by wet impregnation method with consecutive Cu/Zn/adsorbent ratio of 15/5/80 (%wt). The composition of Cu/Zn/adsorbent can be seen in Table 1.

Table 1. Cu/Zn/adsorbent composition.

Compound	Sampel Weight (g)
$Cu(NO_3)_2.3H_2O$	8.55
$ZnSO_4.7H_2O$	3.30
POFA-activated	12

The weighed $Cu(NO_3)_2.3H_2O$ and $ZnSO_4.7H_2O$ metals were dissolved in a beaker glass containing 10 mL of distilled water, then the mixture was stirred using a magnetic stirrer at room temperature for 1 hour until the mixture became homogeneous.

Adsorbent Soaking Process (Wet Impregnation)

POFA activated samples with three variations were then impregnated using the wet impregnation method using Cu metal and Zn promoter. Wet impregnation was carried out by immersing 12 grams of activated POFA in a beaker containing 20 mL of distilled water, then stirring with a magnetic stirrer, then the previously prepared $Cu(NO_3)_2.3H_2O$ and $ZnSO_4.7H_2O$ impregnation solution was dripped slowly into the beaker. The mixture was then stirred using a magnetic stirrer in a beaker covered with aluminum foil at room temperature for 24 hours so that Cu and Zn metal would be absorbed by the activated POFA surface. After 24 hours, the temperature was increased to 60℃ and heated for 3 hours uncovered while continuously stirring using a magnetic stirrer with the aim of reducing the water content and then filtered using filter paper.

Calcination of Samples

Samples that still contain water need to be dried at 105℃ for 16 hours using an oven until the water content dries. After drying, the sample was calcined in a furnace at 350℃ for 3 hours using a porcelain cup. Then samples of POFA-modified 1, POFA-modified 2, and POFA-modified 3 were obtained with varying heating times of 90, 150, and 210 minutes, respectively. The modified POFA adsorbent was then characterized by BET, SEM-EDX, FTIR, and XRD. In BET analysis, the sample is degassed at a temperature of 350°C for 3 hours to measure the adsorption-desorption porosity and determine the surface area and porosity of the sample. In SEM-EDX analysis, the sample is observed at 5000 times magnification and the elements contained in the sample are observed. FTIR analysis was carried out in the long wave range 4000-650 cm^{-1}. Analysis using X-ray diffraction (XRD) was carried out with Cu radiation at a scanning speed of 1/min (step size 0.02) in the 2θ range from 10° to 80°.

Adsorption of β-Carotene from CPO Using Modified POFA Adsorbent

First, the β-carotene content in CPO was analyzed. Adsorption was carried out in batch using the immersion method for three variations of adsorbent, namely POFA-modified 1, POFA-modified 2, and POFA-modified 3. The ratio between adsorbent and CPO was 1:3 (w/v) which was made in a glass beaker. The adsorption process lasted for 2 hours and was heated at a temperature of 60°C using a hot plate while continuously stirring using a magnetic stirrer at a speed of 120 rpm. Once complete, the mixture was filtered using Whatman No.1 filter paper to separate the filtrate and adsorbent. The filtrates that have been obtained, namely POFA-adsorption 1, POFA-adsorption 2, and POFA-adsorption 3 are then put into plastic

bottles and tested to determine the residual β-carotene content in CPO using a UV-VIS spectrophotometer. The largest amount of β-carotene is found at a wavelength of 446 nm, so measurements are carried out at this wavelength.

RESULTS AND DISCUSSION

The POFA-modified used in this study allows for the absorption of β-carotene from CPO. To remove contaminants, enlarge pores and increase surface area, physical activation is carried out by means of size reduction and heating. Meanwhile, for chemical activation, the sample was dipped in a 9% H_3PO_4 solution to remove impurities, increase the Si/Al ratio, and strengthen the adsorbent structure (Lestari, 2010). Adsorption of β-carotene on CPO used three variations of POFA-modified, namely POFA-modified 1, POFA-modified 2, and POFA-modified 3. The adsorbance value was calculated as a function of the β-carotene content in CPO.

Surface Area Analyzer Results

The Branauer-Emmett-Teller (BET) method was used to calculate the specific surface area used Quantachrome Novatouch LX-4 SAA to perform BET analysis for POFA-modified.

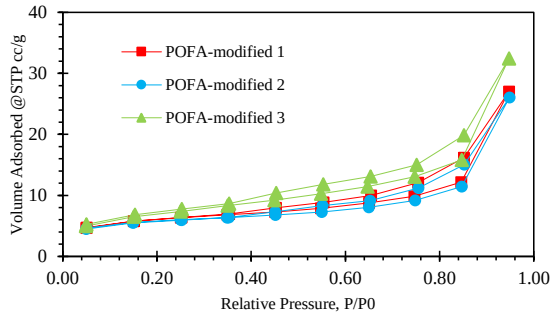

Figure 1. Nitrogen adsorption desorption isotherm curve.

In Figure 1, it can be seen that a small amount of gas is adsorbed at a pressure of P/Po = 0, but when the pressure is increased more than 0.1, gas adsorption occurs, saturating the monolayer (Darmansyah et al., 2016). At intermediate pressures multilayer adsorption occurs and when the pressure is increased capillary condensation occurs on the mesoporous surface characterized by the presence of hysteresis loops. The adsorption isotherm of POFA-modified (Figure 1) shows a type IV N_2 adsorption isotherm according to the IUPAC classification. The type IV isotherm illustrates that this isotherm is compatible with mesoporous solids. It is characterized by a hysteresis loop and high saturation at p/p0 = 0.4 – 0.95. The hysteresis loop in the isotherm is caused by capillary condensation occurring in the mesopores by increasing the relative pressure. The adsorption hysteresis loop of POFA-modified shows an H-3 type loop. This indicates the condensation of adsorbate in the capillary space between parallel plates or open slit-shaped capillary (Yurdakal et al., 2019).

Using the BJH (Barret, Joiner, Halenda) approach, the modified POFA pore size features were also seen from the pore size distribution graph data on Figure 2.

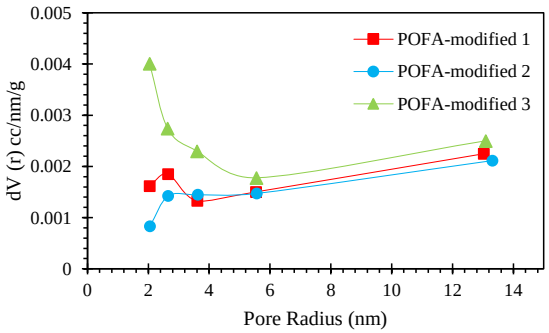

Figure 2. Pore size distribution curve.

Microporous materials are materials whose pore diameter is < 2 nm, mesoporous materials are materials whose pore diameter is 2 – 50 nm, and macroporous materials have a pore diameter > 50 nm (Marsh & Reinoso, 2006). The pore distribution data in Figure 2 shows that the hysteresis in the adsorbent is caused by the presence of meso-sized pores. This is shown in the pore size distribution graph where the pore size is in the mesoporous area, namely at a pore radius of 2 – 14 nm or a diameter of 4 – 28 nm.

The relationship between pore volume and pore size for POFA-modified samples can be observed in Table 2, where a larger pore volume corresponds to a smaller pore size. While pore size has an impact on the selectivity of molecules that will enter the pore, pore volume determines the capacity of adsorbed compounds. The molecules that can be adsorbed also become smaller as the pore volume decreases.

From Table 2 it can be seen that fly ash after activation and impregnation of Cu and Zn metals has a large surface area, which is 19.48 m^2/g in POFA-modified 1. POFA that has not been

Table 2. BET Analysis of POFA-modified surface area.

Sample	Heating Time (min)	BET (m^2/g)	Total Pore Volume (cc/g)	Average Pore Size (nm)
POFA-modified 1	90	19.4785	0.0419052	4.30272
POFA-modified 2	150	18.0175	0.0404099	4.48563
POFA-modified 3	210	13.2363	0.0502714	4.18957

modified, which is 29.1 m^2/g (Kongnoo et al., 2017). Metal loading causes a decrease in the surface area of POFA. This decrease can be caused by some pores that are blocked by the presence of oxide functional groups that occur during H_3PO_4 activation treatment and Cu/Zn metal loading so that N_2 molecules cannot move to the adsorptive site, this is in line with research conducted by (Hosseini et al., 2015).

As seen in Table 2 after modification, the surface area of fly ash decreased. This means that the surface area of the adsorbent is affected by the duration of the heating step in the activation process, but not the pore diameter or volume which does not change significantly. The reduction of surface area, total pore volume, micro and mesopore volume depends on the amount of metal loaded (Hosseini et al., 2015).

Fourier Transform Infared (FTIR) Analysis Results

For the purpose of predicting molecular structure, FTIR (Fourier Transform Infra Red) analysis was used to identify atom-to-atom bonds and find functional groups in POFA samples.

FTIR analysis was carried out in the wavelength range 4000-650 cm^{-1}. FTIR analysis was carried out before and after modification of POFA with H_3PO_4 activator and impregnation of $Cu(NO_3)_2.3H_2O$ metal with $ZnSO_4.7H_2O$ promoter. FTIR wavelength spectra of each POFA sample before and after modification (variation of heating time in the activation process for POFA-modified 1, POFA-modified 2, and POFA-modified 3) is shown in Figure 3.

Figure 3 shows the spectrum from FTIR analysis which shows specific aluminosilicate groups including -OH, Si-H, Al-O, SiO, and Si-O-Si, with wavelengths of 3280.06 and 3615.52 cm^{-1} ; 2087.31 and 1968.03 cm^{-1} ; 1408.93 and 1625.12 cm^{-1} ; 1021.29 and 1028.75 cm^{-1}, and 790.20 cm^{-1}. Determination of characteristic group for each unmodified and modified POFA sample will be explained in Table 3.

Based on Table 3 which shows POFA-modified, there are POFA absorption bands in successive waves, namely 3280.06; 3615.52; and 3280.06 cm^{-1}. This shows that there is stretching vibration of the O-H group which is loaded with adsorbed water molecules. POFA contains Si-H

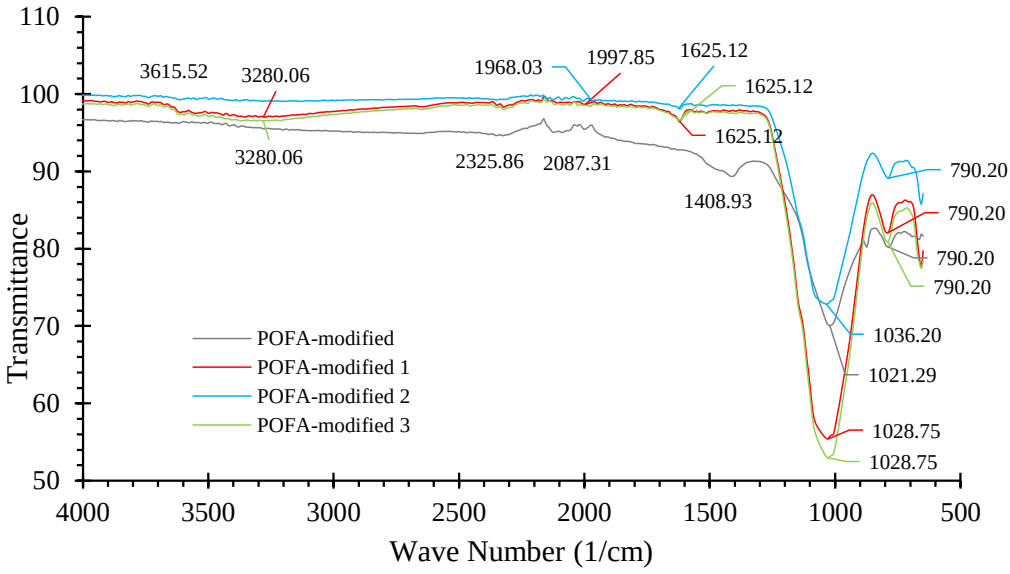

Figure 3. FTIR analysis results.

Table 3. FTIR wavenumber of POFA samples.

Characteristic Group	POFA (cm^{-1})	POFA-modified 1 (cm^{-1})	POFA-modified 2 (cm^{-1})	POFA-modified 3 (cm^{-1})
-OH Group	-	3280.06	3615.52	3280.06
-Si-H stretching	2087.31 -2325.86	1997.85	1968.03	-
Al-O stretching	1408.93	1625.12	1625.12	1625.12
Si-O asymmetric stretching	1021.29	1028.75	1036.20	1028.75
Si-O-Si bending	790.20	790.20	790.20	790.20

groups which can be seen in the absorption band 2087.31 – 1968.03 cm^{-1} (Hardjono, 1992). In the POFA structure connected with Si-OH groups, the wave number 1021.29 – 1028.75 cm^{-1} widens and intensifies sharply, indicating asymmetric Si-O stretching vibrations. To reduce the crystal phase in the POFA structure, the peak width reveals the number of Si-OH groups. POFA has a pore structure, proven by the bending vibration of Si-O-Si at an absorption of 790.20 cm^{-1} (Lesbani & Mohadi, 2014; Zhirong et al., 2011). In POFA-unmodified, the wave number changes with the modification of various heating times during the activation process, as shown in Figure 3 and Table 3. Each has essentially the same peak; however, some undergo wavenumber modification. In POFA-modified, -OH stretching vibrations appear from H_2O in the wave number range of 3280.06 cm^{-1} to 3615.52 cm^{-1} and 3280.06 cm^{-1}.

The stretching vibration of the -OH group is described in the wave number range 3700 - 3200 cm^{-1}, according to (Socrates, 1995). The POFA framework forms hydrogen bonds with silica due to the presence of -OH groups. The decrease in the number of water molecules absorbed in the POFA interlayer is indicated by a shift towards a higher wave number. However, the -OH stretching vibration experienced a smaller decrease in wave number between POFA-modified 2 with heating for 150 minutes and POFA-modified 3 with heating for 210 minutes, from 3615.52 cm^{-1} to 3280.06 cm^{-1}. This indicates a weak -OH bond. This event shows that H_3PO_4 can reduce the interaction of -OH groups with impurities, so that impurities can be removed and POFA pores become cleaner (Irawan et al., 2014). The Si-H group in POFA is depicted in Figure 3 through its spectral appearance at wavelengths 2087.31 – 2325.86 cm^{-1}, 1997.85 – 2368.65 cm^{-1}, and 1968.03 cm^{-1}. The Si-H POFA-modified 3 absorption band may not exist because the absorption intensity of the material in that region is too low to be detected by the IR spectrum (Rosyidah, 2008). The wave number 1408.93 cm^{-1} shows the Al-O stretching vibration in the POFA, while the wave number 1625.12 cm^{-1} shows changes in the POFA-modified. the Al-O group in POFA can be found at the absorption peak of 470-1650 cm^{-1} (Lin et al., 2020). POFA and POFA-modified show different spectral absorption bands, with an absorption area of 1625.12 cm^{-1} shifted away from the wave number 1408.93 cm^{-1}. The resulting changes indicate a slow interaction between the Al-O groups. Because the shift is always within the limits of the infrared absorption zone, which never changes, it has little effect on the micromolecular structure (Hardjono, 1992). Figure 3 shows that the asymmetric stretching vibration of Si-O POFA experienced a downward shift in wave number, from 1021.29 cm^{-1} to 1028.75 cm^{-1} to 1036.20 cm^{-1} to 1028.75 cm^{-1}, which is POFA dealumination. Dealumination can be seen spectroscopically at wave numbers 300-1425 cm^{-1} (Rosyidah, 2008). According to (Sastrohamidjojo, 1992), the bending vibration of Si-O-Si is in the absorption band 770 cm^{-1} - 1035 cm^{-1}, and the wave number that occurs in the absorption band 790.20 indicates the existence of this vibration.

X-Ray Diffraction (XRD) Characterization Results

XRD analysis was conducted using a Bruker D2 Phaser to determine the crystalline phase. XRD analysis was conducted using a Bruker D2 Phaser to determine the crystalline phase, the amount of crystalline phase, and amorphous material contained in fly ash that had been activated using H_3PO_4 and impregnated using Cu/Zn metal.

Modified fly ash is not reduced by H_2 gas, so the diffraction pattern of modified fly ash still contains metal oxides, such as CuO and ZnO. This is because the impregnation of Cu metal in $Cu(NO_3)_2.3H_2O$ undergoes a decomposition reaction into CuO in accordance with the reaction equation in (Nasikin et al., 2004).

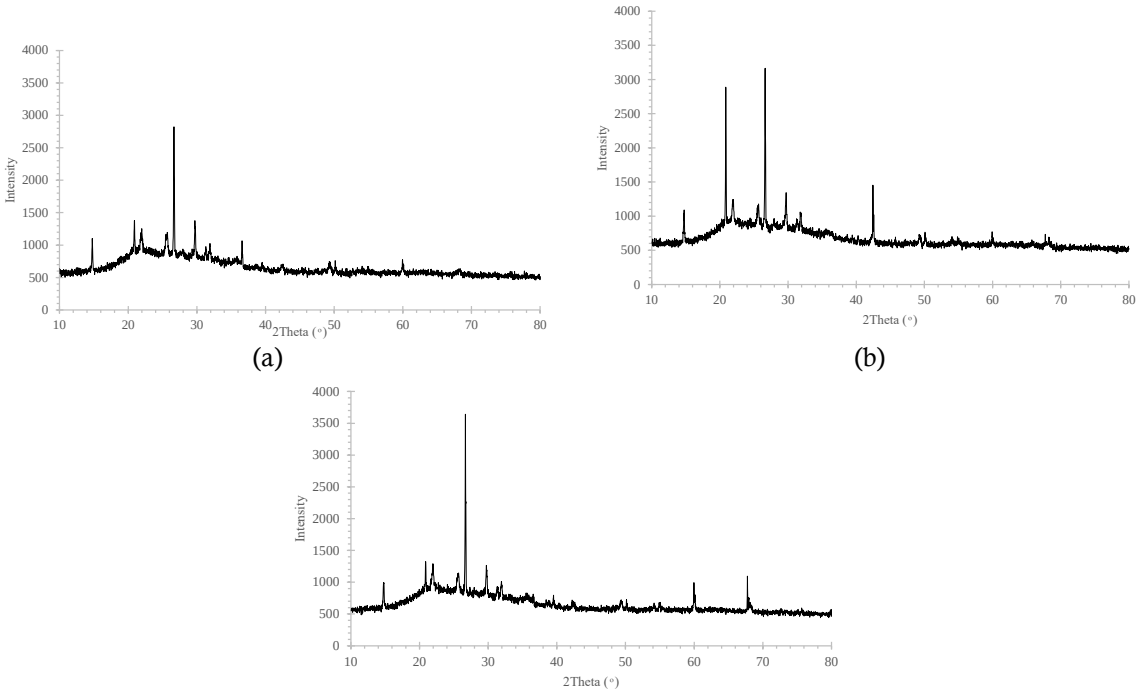

Figure 4. XRD analysis results (a) POFA-modified 1; (b) POFA-modified 2; (c) POFA-modified 3.

$$Cu(NO_3)_2.3H_2O \rightarrow Cu(NO_3)_2 + 3H_2O \quad (1)$$

$$2Cu(NO_3)_2 \rightarrow 2CuO + 4NO_2 + O_2 \quad (2)$$

In addition, the impregnation of Zn metal in $ZnSO_4.7H_2O$ undergoes a decomposition reaction into ZnO according to the reaction equation in the research of (Istadi et al., 2012).

$$ZnSO_4.7H_2O \rightarrow ZnO + H_2SO_4 + 6H_2O \quad (3)$$

In Figure 4, It can be seen that modified POFA which has been analyzed using XRD shows characteristic peaks of crystalline phases, namely CuO, ZnO, quartz and mullite (especially silicon oxide (SiO_2)). The CuO diffraction peak will be visible at an angle of 2θ, namely 20.76°; and 42.48° (Peternela et al., 2017). The diffraction peak of ZnO will be visible at angle of 2θ, namely 31.75° (Iqbal et al., 2014). The diffraction peak at angle of 2θ, namely 26.75°, comes from the quartz mineral content (Higgins & Treacy, 2007). In addition, the peak located at an angle of 2θ, namely 39.7°, comes from SiO_2 mullite crystals (Islam et al., 2015). The diffraction peaks of each crystal phase in POFA-modified are explained in Table 4.

The main diffraction peak of CuO is located at an angle of around 20°, while the ZnO diffraction peak is located at an angle of around 31° which can be seen based on Table 4. This result is in accordance with research conducted by where the CuO peak forms an angle of 20.76° and also research by (Greeshma et al., 2021) which shows the ZnO peak forms an angle of 31.82°. The CuO diffraction peak intensity for the POFA-modified 2 sample at an angle of 2θ is 2887, this shows that the CuO metal content in the POFA-modified 2 sample is higher than the other 2 samples. The ZnO crystal phase was also found in all samples, this shows that the impregnation treatment on the POFA samples will form a new crystal phase in POFA.

Cu can react with the middle double bond of β-carotene. The cause is the increase in electrostatic attraction between β-carotene and Cu. However, high temperatures can quickly deactivate Cu metal. This problem can be overcome by adding Zn to Cu which functions as a promoter. Therefore, Zn metal works to stop Cu from becoming inactive at high temperatures (Hosseini et al., 2015). With the new crystal phases of CuO and ZnO formed, it can increase the b-carotene adsorption ability of CPO. POFA which has a large silica content here acts as a support for the Cu metal catalyst which acts as an active site for the absorption of β-carotene.

The highest peak of the POFA sample is at a 2θ angle of around 26° which has a peak intensity of 2824 to 3643, this indicates the formation of quartz produced (Higgins & Treacy, 2007). All

Table 4. Diffraction Pattern of Modified POFA

Crystal Phase	POFA-modified 1		POFA-modified 2		POFA-modified 3	
	2θ (°)	I (a.u)	2θ (°)	I (a.u)	2θ (°)	I (a.u)
CuO	20.921	1382	20.866	2887	20.888	1325
	42.419	678	42.452	1399	42.380	701
ZnO	31.916	1020	31.846	1038	31.917	1006
Quartz	26.677	2824	26.632	3118	26.679	3643
SiO2	39.523	729	39.423	716	39.497	762

samples have a quartz crystal phase, this could be caused by the remaining POFA material which might contribute to the appearance of the quartz peak. In the POFA-modified sample preparation method, the prepared POFA is mixed directly with the H_3PO_4 solution and impregnated with Cu/Zn metal, this results in any quartz from the raw material always being carried in the POFA samples in this study. This quartz crystal component is a very sTable crystal phase (Freire et al., 2020). The SiO_2 crystal phase was also found in the modified POFA samples. POFA samples have a large silica content, which is the cause of the appearance of a crystalline phase in all POFA-modified samples. In addition, using H_3PO_4 solution as an activator can combine with mullite and quartz grains which can produce SiO_2 (Kotova et al., 2022).

Analysis Result Scanning Electron Microscopy-Edx (SEM-EDX)

SEM analysis was conducted to determine the morphology of the adsorbent formed. While EDX analysis aims to determine the elemental content in the adsorbent.

The modified POFA has a rough and round surface, as can be seen in Figure 5. SEM analysis results with 5000 times magnification. Before modification, POFA contained an aluminosilicate (Si-Al) component, as seen in spherical particles (White & Case, 1990). These particles will eventually undergo activation to produce particles that are more porous and coarser, making them more useful as adsorbents. Fine and aggregated Cu/Zn metal particles can be observed on the POFA surface (Figure 5). Aggregates of Cu/Zn metal particles are clearly visible and loaded on fly ash which appears as white particles on the surface of POFA. The results of EDX analysis prove that there is Cu/Zn element content in modified POFA as shown in Table 5.

The results of EDX analysis proved that there are Cu/Zn elements in POFA-modified. And the content of POFA-modified adsorbent that has been activated with H_3PO_4 and Cu/Zn impregnation.

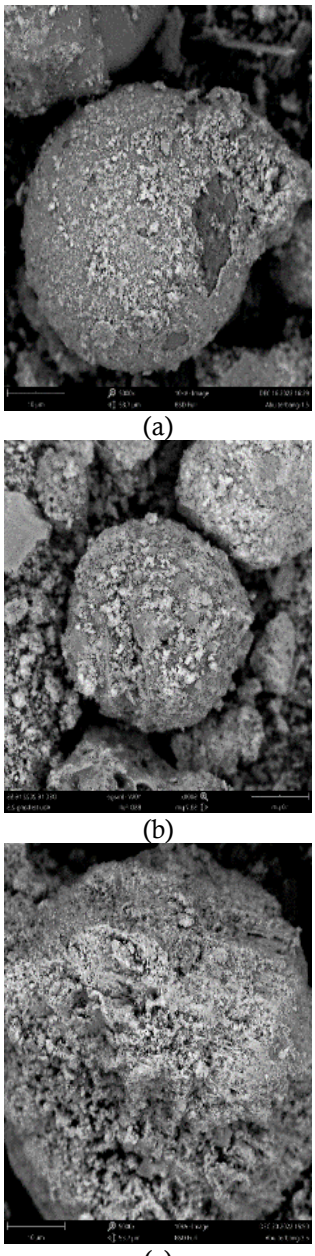

(a) (b) (c)

Figure 5. SEM analysis results magnification 5000 times (a) POFA-modified 1 (b) POFA-modified 2 (c) POFA-modified 3.

Table 5. Diffraction pattern of modified POFA

Composition	POFA-modified 1	POFA-modified 2	POFA-modified 3
Si	19.26	22.53	37.53
O	46.03	36.13	37.27
Cu	4.98	15.29	3.24
Zn	-	6.63	-
C	1.82	-	5.22
N	8.39	6.95	10.22
Fe	1.50	0.63	0.24
K	4.77	2.07	2.90
Ca	2.89	1.75	0.64
Na	2.05	5.59	0.52
Al	2.24	0.23	0.86
P	3.57	2.21	0.90
Mg	2.50	-	0.47
Total	**100**	**100**	**100**

As can be seen in Table 5, there are several elements contained in the modified POFA. During the activation process, metal oxide compounds do not come out of the support pores. The metal oxide compound remains bound to the pores of the support until the Cu and Zn metal impregnation process occurs (Fauziah, 2009). However, the impurity content in the modified POFA decreased and the Si/Al ratio increased. This is because activation can increase the silica (Si) content and reduce the aluminum (Al) content, which means the Si/Al ratio increases (Faradilla et al., 2016). With reduced impurities such as Fe, K, Ca, Na, Al, P, and Mg, the mass fraction of other elements required will be greater as can be seen in Table 5.

The Cu element content was obtained from the impregnation of Cu and Zn metal. However, the Zn element content is only found in POFA with a 150 minute heating variation, namely POFA-modified 2, whereas it is not found in other variations. The H_3PO_4 activator in POFA can be the cause of the closure of the ZnO promoter molecule (Tsani, 2011). In the heating process, activation still leaves the H_3PO_4 activator in POFA. This can result in the ZnO metal being covered with H_3PO_4 when stirring the POFA-activated Cu/Zn solution during the impregnation process. In POFA-modified there is Zn which shows that only a small amount of H_3PO_4 remains in the activation process so it does not cover all the ZnO metal.

UV-Vis Spectrophotometric Analysis

UV-Vis spectrometers perform on the basis that molecules can be stimulated from low energy levels to higher energy levels by absorbing visible light into ultraviolet light. In this study a modified POFA adsorbent was used to adsorb β-carotene from CPO. In Figure 6, The color can be seen in the pure β-carotene sample which has been dissolved in n-hexane and pure CPO.

(a) (b)

Figure 6. (a) n-hexane solubilized pure β-carotene (b) pure CPO.

In Figure 6 (a), the pure β-carotene sample that has been dissolved using n-hexane solvent is seen to have a bright yellow color, and there are still β-carotene solids that have not been dissolved. And in Figure 6 (b) the CPO sample is seen to have an orange yellow color. After the adsorption process, pure CPO samples and CPO samples that have been adsorbed using POFA-modified 1, POFA-modified 2, and POFA-modified 3 were weighed as much as 0,1015 g and dissolved using n-hexane solvent in a 25 mL measuring flask until the limit mark.

In Figure 7 (a) the color of CPO is still dark red because the concentration of β-carotene is still quite high at 792.41 ppm. The capacity of POFA-

modified to absorb β-carotene colorant is explained by the color change in the CPO. The absorbance value was measured in this test using a UV-Vis spectrophotometer.

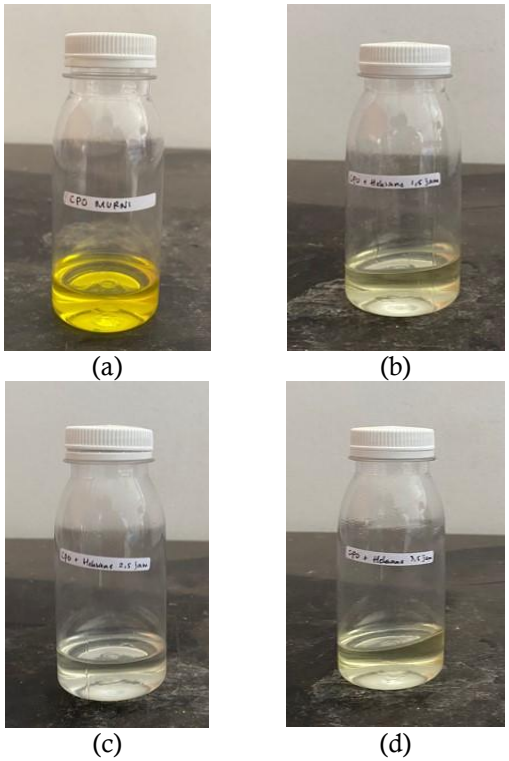

(a) (b)

(c) (d)

Figure 7. Color change in CPO a) before adsorption b) POFA-modified 1 c) POFA-modified 2 d) POFA-modified 3.

The following equation was used to calculate the concentration of β-carotene in the sample after the adsorbance value (A) was obtained from the analysis.

$$\beta - Karoten = \frac{383 \times Adsorbance\ on\ the\ sample}{Sample\ weight} \times 0.25 \quad (3)$$

Adsorbance and beta carotene value calculation results obtained from CPO samples using the above equation can be seen in Table 6.

β-carotene levels in CPO samples can be determined using the resulting absorbance values. Based on these findings, it is known that the POFA-modified 2 sample which has a β-carotene content of 116.98 ppm compared to other samples has the lowest levels. The POFA-modified 2 sample succeeded in absorbing β-carotene levels of 86%, while POFA-modified 1 and POFA-modified 3 succeeded in absorbing β-carotene levels of 84% and 80%, respectively. This shows that compared to other variations, the adsorbent with a heating time variation of 150 minutes when activation process has the best β-carotene adsorption capacity. Adsorption of β-carotene using modified POFA adsorbent occurs on the surface of POFA-modified which already contains the active Cu site. Because the average pore size of the POFA-modified produced is 4 nm, the adsorption process of β-carotene which has a pore diameter of 17 nm only occurs on the POFA surface. Cu can bind to β-carotene due to the increase in electrostatic attraction between β-carotene and Cu. POFA containing silica-alumina here acts as a support for the Cu metal catalyst which acts as an active site for the absorption of β-carotene. Silica-alumina has a large surface area and pore diameter so it can be used as a Cu catalyst support.

CONCLUSION

From the results, the research concluded that POFA can be used as an adsorbent for the absorption of β-carotene in Crude Palm Oil (CPO). All POFA-modified samples have mesopore size. XRD analysis showed that the diffraction pattern of CuO, ZnO, quartz, and SiO_2. POFA has O-H group, -Si-H stretching vibration, Al-O vibration, Si-O asymmetric stretching vibration, and Si-O-Si bending vibration. Based on the results of UV-Vis Spectrophotometry analysis, the best results were obtained in the β-carotene adsorption process with POFA-modified 2 variations of activation heating time for 150 minutes, which obtained a β-carotene absorption value of 116.98 ppm or successfully absorbed 86%. Due to the limitations of the research, further research can conduct various of adsorption conditions such as temperature, time,

Table 6. Calculation results of UV-Vis spectrophotometric analysis.

Sample Code	Sample Weight (g)	Absorbance (A)	β-carotene after adsorption (ppm)	Adsorption (%)
POFA-modified 1	0.1015	0.136	128.30	84
POFA-modified 2	0.1015	0.124	116.98	86
POFA-modified 3	0.1015	0.168	158.48	80

and CPO concentration to see the adsorption ability of H_3PO_4-activated POFA and Cu/Zn impregnation in adsorbing β-carotene on CPO. Further research can conduct research on β-carotene desorption.

REFERENCES

Choo, Y. M. 2000. Specialty products: carotenoids.

Darmansyah, D., Saputra, H., Ginting, S., Ardiana, L. 2016. Synthesis and Characterization of Mcm-41 from Coal Fly Ash for Tapioca Wastewater Treatment. ARPN Journal of Engineering and Applied Sciences. 11(7): 4772–4777.

Elly, K. 2008. Pemanfaatan cangkang kelapa sawit sebagai arang aktif. Jurnal Penelitian Ilmu-Ilmu Teknik. 8(2): 96–103.

Faradilla, A. R., Yulinawa, H., Suswantoro, E. 2016. Pemanfaatan fly ash sebagai adsorben karbon monoksida dan karbon dioksida pada emisi kendaraan bermotor. Prosiding Seminar Nasional Cendekiawan. 1(2016): 1–2.

Fauziah, N. 2009. Pembuatan arang aktif secara langsung dari kulit acacia mangium wild dengan aktivasi fisika dan aplikasinya sebagai adsorben. Undergraduate Theses. IPB University.Bogor, Indonesia.

Freire, A. L., Moura-Nickel, C. D., Scaratti, G., De Rossi, A., Araújo, M. H., Júnior, A. D. N., Rodrigues, A. E., Castellón, E. R., Moreira, R. de F. P. M. 2020. Geopolymers produced with fly ash and rice husk ash applied to CO_2 capture. Journal of Cleaner Production. 273: 122917.

Gao, Y., Kispert, L. D. 2014. A DFT study of the interaction between olefins and Cu^{2+} on silica and MCM-41 model surfaces. Dalton Transactions. 43(16): 6221–6228.

Greeshma, K. P., Muthulingam, S., Thamizselvi, R., Sen, D. B. 2021. Antimicrobial studies and characterization of ZnO nanoparticles by chemical method. GSC Advanced Research and Reviews. 8(2): 71–77.

Harahap, I. S., Wahyuningsih, P., Amri, Y. (2020). Analisa kandungan beta karoten pada CPO (Crude Palm Oil) di pusat penelitian kelapa sawit (PPKS) Medan menggunakan spektrofotometri UV-Vis. QUIMICA: Jurnal Kimia Sains Dan Terapan. 2(1): 9–13.

Hardjono, S. 1992. Infrared Spectroscopy. Spektroskopi Inframerah), Yogyakarta, Liberty.

Higgins, J. B., Treacy, M. M. J. 2007. Collection of simulated XRD powder patterns for zeolites. Elsevier Science & Technology.

Ho, W. W. S., Ng, H. K., Gan, S. 2012. Development and characterisation of novel heterogeneous palm oil mill boiler ash-based catalysts for biodiesel production. Bioresource Technology. 125: 158–164.

Hosseini, S., Bayesti, I., Marahel, E., Babadi, F. E., Abdullah, L. C., Choong, T. S. Y. 2015. Adsorption of carbon dioxide using activated carbon impregnated with Cu promoted by zinc. Journal of the Taiwan Institute of Chemical Engineers. 52: 109–117.

Iqbal, M., Marintan, E., Septiani, N. L. W., Suyatman, S., Nuruddin, A., Nugraha, N., Yuliarto, B. 2014. Synthesis and harmful gas sensing properties of zinc oxide modified multi-walled carbon nanotubes composites. Advanced Materials Research. 1044: 172–175.

Irawan, C. 2013. Adsorpsi Ion Fe^{2+} Menggunakan Adsorben Abu Layang Batubara. Undergraduate Theses. Universitas Brawijaya. Malang, Indonesia.

Irawan, C., Atikah, A., Rumhayati, B. 2014. Adsorption of Iron by Fly Ash Adsorbent of Coal. The Journal of Pure and Applied Chemistry Research. 3(3): 88.

Islam, S., Riaz, S., Rahman, R. A., Naseem, S., Ottoman, Z. 2015. Structural and dielectric properties of boron-doped and un-doped mullite thin films. Journal of Sol-Gel Science and Technology. 74: 368–377.

Istadi, I., Anggoro, D. D., Buchori, L., Utami, I., Solikhah, R. 2012. Process parameters optimization of potential SO42-/ZnO acid catalyst for heterogeneous transesterification of Vegetable oil to biodiesel. Bulletin of Chemical Reaction Engineering & Catalysis. 7(2): 150–157.

Kongnoo, A., Tontisirin, S., Worathanakul, P., Phalakornkule, C. 2017. Surface characteristics and CO_2 adsorption capacities of acid-activated zeolite 13X

prepared from palm oil mill fly ash. Fuel. 193: 385–394.

Kotova, O. B., Ustyugov, V. A., Sun, S., Ponaryadov, A. V. 2022. Mullite production: phase transformations of kaolinite, thermodynamics of the process. Записки Горного Института. 254: 129–135.

Lesbani, A., Mohadi, R. 2014. Brönsted acid of Keggin type polyoxometalate catalyzed pinacol rearrangement. Bulletin of Chemical Reaction Engineering & Catalysis. 9(2): 136–141.

Lestari, D. Y. 2010. Kajian modifikasi dan karakterisasi zeolit alam dari berbagai negara. Prosiding Seminar Nasional Kimia Dan Pendidikan Kimia. 30(1): 1–6.

Lin, W. Y., Prabhakar, A. K., Mohan, B. C., Wang, C.-H. 2020. A factorial experimental analysis of using wood fly ash as an alkaline activator along with coal fly ash for production of geopolymer-cementitious hybrids. Science of the Total Environment. 718: 135289.

Marsh, H., Reinoso, F. R. 2006. Activated carbon. Elsevier.

Nasikin, M., Eliyanti, A., Arto, D. 2004. Karakterisasi katalis $CuO/ZnO/Al_2O_3$ dengan temperature programmed desorption (TPD). Jurnal Teknologi. XVIII (2).

Okogeri, O., Okoro, B. 2014Storage stability and sensory attributes of crude palm oil adulterated with red dye. European Journal of Agriculture and Forestry Research. 2(1): 10–17.

Peternela, J., Silva, M. F., Vieira, M. F., Bergamasco, R., Vieira, A. M. S. 2017. Synthesis and impregnation of copper oxide nanoparticles on activated carbon through green synthesis for water pollutant removal. Materials Research. 21: e20160460.

Rahayu, E., Luna, P., Usmiati, S., Sunarmani, S. 2021. Optimasi Sintesis dan Aplikasi Adsorben dari Limbah Ekstraksi Biosilika Sekam Padi. Indonesian Journal of Industrial Research. 38(1): 36–45.

Rangkuti, I. U. P., Purwanto, H., Pohan, H. S. U. 2021. Pengaruh Jenis Aktivator Adsorben Abu Boiler Pabrik Kelapa Sawit Terhadap Mutu Minyak Sawit Mentah. Jurnal Teknik Pertanian Lampung. 10(3): 351–355.

Rasmawan. 2009. Pemanfaatan Limbah Pabrik Sawit Untuk Pakan Ternak Sapi Di Bengkulu. https://uwityangyoyo.wordpress.com/2009/05/16/pemanfaatan-limbah-pabrik-sawit-untuk-pakan-ternak-sapi-di-bengkulu/

Rosyidah, H. 2008. Studi kinetika adsorpsi merkuri (II) pada biomassa daun enceng gondok (Eichhornia crassipes) yang diimmobilisasip ada matriks polisilikat. Undergraduate Theses. Universitas Islam Negeri Maulana Malik Ibrahim. Aceh, Indonesia.

Sastrohamidjojo, H. 1992. Infrared spectroscopy. Sarjoko, 1sted. Liberty, Yogyakarta.

Shofa. 2012. Preparation of activated carbon from sugarcane bagasse by potassium hydroxide activation [Universitas Indonesia]. https://lib.ui.ac.id/detail?id=20311088&lokasi=lokal

Socrates, G. 1995. Infrared characteristic group frequencies: Tables and charts.

Tsani, F. 2011. Preparasi dan Karakterisasi Katalis $NiMo/\gamma\text{-}Al_2O_3$ untuk Sintesis Bahan Bakar Bio dari Minyak Jarak Melalui Pirolisis Berkatalis. Depok: Teknik Kimia Universitas Indonesia.

Wardhani, O. P., Aini, N. 2016Adsorpsi β-Karoten Yang Terkandung Dalam Minyak Kelapa Sawit (Crude Palm Oil) Menggunakan Karbon Aktif. Jurnal Teknik Kimia USU. 5(1): 52–57.

White, S. C., Case, E. D. 1990. Characterization of fly ash from coal-fired power plants. Journal of Materials Science. 25: 5215–5219.

Yahya, Z., Abdullah, M., Hussin, K., Ismail, K. N., Sandu, A. V., Vizureanu, P., Razak, R. A. 2013. Chemical and physical characterization of boiler ash from palm oil industry waste for geopolymer composite. Revista de Chimie. 64(12): 1408–1412.

Yurdakal, S., Garlisi, C., Özcan, L., Bellardita, M., Palmisano, G. 2019. (Photo) catalyst characterization techniques: adsorption isotherms and BET, SEM, FTIR, UV–Vis, photoluminescence, and electrochemical characterizations. In Heterogeneous photocatalysis (pp. 87–152). Elsevier.

Zhirong, L., Uddin, M. A., Zhanxue, S. 2011. FT-IR and XRD analysis of natural Na-bentonite and Cu (II)-loaded Na-bentonite. Spectrochimica Acta Part A: Molecular and Biomolecular Spectroscopy. 79(5): 1013–1016.